2019

Evaluation of Silver Nanoparticle Encapsulation in DPPC-Based Liposome By Different Methods For Enhanced Cytotoxicity

Azeez O. Yusef
Technological University Dublin

Alan Casey
Technological University Dublin, alan.casey@tudublin.ie

Recommended Citation

Yusef, A.O. and Casey, A. (2019). Evaluation of silver nanoparticle encapsulation in DPPC-based liposome by different methods forenhanced cytotoxicity. International Journal of Polymeric Materials , June 2019 doi:10.1080/00914037.2019.1626390

GPOM#1626390, VOL 0, ISS 0

Evaluation of silver nanoparticle encapsulation in DPPC-based liposome by different methods for enhanced cytotoxicity

Azeez O. Yusuf, and Alan Casey

QUERY SHEET

This page lists questions we have about your paper. The numbers displayed at left are hyperlinked to the location of the query in your paper.

The title and author names are listed on this sheet as they will be published, both on your paper and on the Table of Contents. Please review and ensure the information is correct and advise us if any changes need to be made. In addition, please review your paper as a whole for typographical and essential corrections.

Your PDF proof has been enabled so that you can comment on the proof directly using Adobe Acrobat. For further information on marking corrections using Acrobat, please visit http://journalauthors.tandf.co.uk/production/acrobat.asp; https://authorservices.taylorandfrancis.com/how-to-correct-proofs-with-adobe/

The CrossRef database (www.crossref.org/) has been used to validate the references.

AUTHOR QUERIES

No Queries

INTERNATIONAL JOURNAL OF POLYMERIC MATERIALS AND POLYMERIC BIOMATERIALS
https://doi.org/10.1080/00914037.2019.1626390

Evaluation of silver nanoparticle encapsulation in DPPC-based liposome by different methods for enhanced cytotoxicity

Azeez O. Yusuf[a,b] and Alan Casey[a,b]

[a]School of Physics, Dublin Institute of Technology, Dublin, Ireland; [b]Nanolab Research Centre, FOCAS Research Institute, Dublin Institute of Technology, Dublin, Ireland

ABSTRACT

Here we carried out a comparative study on two cost and time effective methods of encapsulating silver nanoparticles (AgNP) in dipalmitoyl-phosphatidyl choline (DPPC)/cholesterol-based liposome to enhance its cytotoxicity and reduce cytotoxic concentrations and evaluated the effect of this on a blood cell line (THP1 monocytes) often involved in uptake of nanoparticles during human exposure. DLS and Zeta potential analyses over a 6-months period showed the extruded Lipo-AgNP (ExLipo-AgNP) exhibited more stable characteristics when compared with the probe-sonicated Lipo-AgNP (PB-Lipo-AgNP). SEM microscopy indicated agglomeration of the PB-Lipo-AgNP which was not observed in Ex-Lipo-AgNP. Ex-Lipo-AgNP also exhibited higher temperature-dependent stability with 35.3% reduction in size from 20 °C to 37 °C while PB-Lipo-AgNP was less stable exhibiting 55% size reduction over same temperature range. Load release study over 24 h showed a controlled load release from Ex-Lipo-AgNP while the PB-Lipo-AgNP exhibited burst release at pH 4 and 6.5. Interestingly, it was found that Ex-Lipo-AgNP induced significantly higher toxicity on THP1 cell line after 24 h exposure compared with control unexposed cells; uncoated AgNP and PB-Lipo-AgNP exposed cells at the same concentration. Thus, for the first time, we report that liposomal encapsulation of AgNP by extrusion produces a stable nanocapsule with enhanced cytotoxicity, thus preventing overreliance on high AgNP concentration to achieve desired toxicity.

GRAPHICAL ABSTRACT

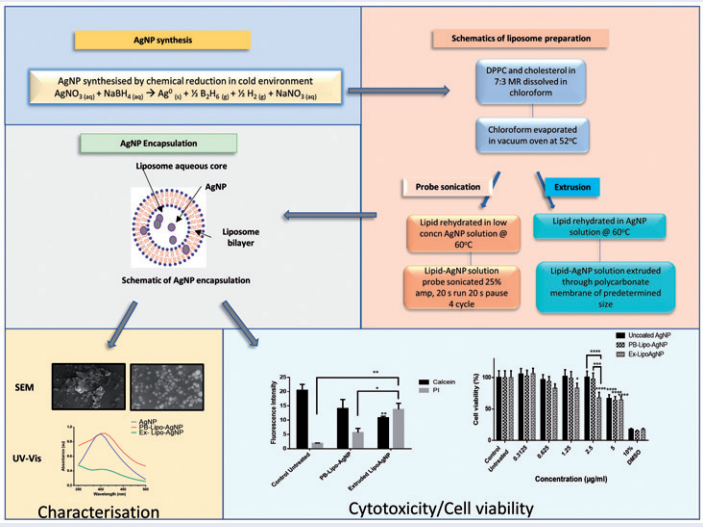

ARTICLE HISTORY
Received 21 March 2019
Accepted 29 May 2019

KEYWORDS
Silver nanoparticle (AgNP); encapsulation; liposome; extrusion

1. Introduction

Silver nanoparticles (AgNP) are a widely used nanoparticle for its antibacterial activities and many of the already commercialized products contain AgNP in high concentrations as the active ingredient. For example, AgNP is widely used as antibacterial coating on medical garments and surgical equipment and even on food materials to prolong shelf life by preventing food degradation consequent upon bacterial

CONTACT Azeez O. Yusuf Azeez.yusuf1@mydit.ie School of Physics, Dublin Institute of Technology, Kevin Street, Dublin 8, Ireland; Nanolab Research Centre, FOCAS Research Institute, Dublin Institute of Technology, Kevin Street, Dublin 8, Ireland.
Color versions of one or more of the figures in the article can be found online at www.tandfonline.com/gpom.

metabolism and growth[1,2]. In addition, AgNP are currently being investigated by different studies as a chemotherapeutic in cancer treatment[3–6]. Unfortunately, with the rise in the biomedical applications of AgNP, development of adverse conditions due to repeated human exposure to AgNP is imminent either from direct contact with products containing AgNP or AgNP that has leached into the ecosystem. AgNP has been reported to cause several adverse effects such as skin irritation and discoloration, hepatotoxicity, kidney damage, DNA damage and epithelia cell damage[7].

Adverse reactions of conventional drugs are not uncommon and improvement on the delivery mechanisms has been a major way to limit these setbacks. For AgNPs however, there has been little or no research into how to improve upon the delivery mechanism to enhance their antibacterial or anticancer activities. The applications of liposomes in drug delivery systems (DDS) have been studied for more than two decades and there have been significant improvements in the formulations and methods by which liposome are prepared. For instance, phosphatidyl choline (PC) based lipids are highly used in liposome preparation likely due to the fact that PC makes up about 80% of the surfactants found on epithelial lining of human airways and lungs. Interestingly, the majority of the PC in the human airways is present in the form of dipalmitoylphosphatidyl choline (DPPC), and this makes up about 60% of the natural surfactants found in the human airways and lungs[8]. Consequently, DPPC is highly unlikely to elicit immune response when incorporated in a liposomal formulation compared to the other derivatives.

Liposomes are designed to mimic the lipid bilayer of the cell membrane and while the natural bilayer of the cell membrane is made up different phospholipids, they also contain cholesterol molecules that help restrict the movement of the fluid phospholipid molecules. In the same manner, it has been shown that cholesterol, when incorporated in liposomal formulations at the right concentration can produce such rigidity to protect the liposomal content[9]. In this study, AgNP synthesized by chemical reduction of silver nitrate ($AgNO_3$) using sodium borohydride ($NaBH_4$) was encapsulated in a DPPC/cholesterol liposome to both stabilize and improve the uptake of the AgNP *in vitro* for enhanced cytotoxicity. Two simple encapsulation methods were trialed AgNP, followed by nanoparticle characterization and evaluation of cytotoxicity on a THP1 cell line, a monocytic cell line which acts as first line of Defense against nanoparticle during exposure[10].

2. Materials and methods

2.1. Chemicals and reagents

Silver nitrate ($AgNO_3$), sodium borohydride ($NaBH_4$), DPPC, cholesterol, Phorbol 12-myristate 13-acetate (PMA) and propidium iodide (PI) were purchased from Sigma Aldrich, Dublin, Ireland while chloroform, Calcein-AM dye and Alamar blue (AB) were from ThermoFischer Scientific, Dublin, Ireland.

2.2. AgNP synthesis

To synthesize AgNP, 6 mL of 1 mM of $AgNO_3$ solution was added dropwise into an Erlenmeyer flask containing magnetic stirrer a 350 rpm and ice cold 30 mL of 2 mM of $NaBH_4$. The stirring was continued until last drop when the stirrer was removed for the solution to turn golden yellow. The obtained AgNP was characterized by UV/Vis in a Spectramax M2 microplate reader while atomic absorption spectrophotometry (AAS) was employed to monitor silver (Ag) concentration using a SpectrAA200 Varian Spectrophotometer (Mulgrave, VC, Australia). The samples were analyzed with a silver hollow cathode lamp at an operating current of 7.5 mA. Hydrodynamic size of AgNP and liposomal AgNP (Lipo-AgNP) was carried out with Malvern Zetasizer Nano ZS (Malvern Panalytical, Malvern, UK). Nanoparticles were loaded into a prerinsed folded capillary cell up to the marked portion. For zeta potential, an applied voltage of 15 and 50 V was used for Lipo-AgNP and free AgNP respectively.

2.3. Liposome synthesis, AgNP encapsulation and characterization

Liposome was prepared by probe sonication and extrusion methods. DPPC and cholesterol were weighed in a mass ratio such that eventual rehydration of the lipid film obtained will give a 7:3 molar ratio solution respectively. The lipids were dissolved in a fixed amount of chloroform and mixed until the mixture becomes clear. The resulting solution was placed in a vacuum oven set at 52 °C for the chloroform to evaporate.

2.3.1. Probe sonication method

The lipid cake formed was then rehydrated in AgNP solution at 60 °C. AgNP solution were added to the lipid at 1:300 (w/w) of AgNP:DPPC after which the solution was vortexed briefly for 2 min to form multi-lamellar vesicles (MLV). The mixture was probe sonicated at 21% amplitude, 20 s run and 20 s pause for 4 cycles to form Small Uni-lamellar Vesicles (SUV). The resultant mixture was then centrifuged at 800 $\times g$ for 10 min at 4 °C to remove any MLVs. The suspension was subjected to DLS and zeta potential analysis for size and stability measurements respectively.

2.3.2. Extrusion method

The lipid film was rehydrated in AgNP solution at 60 °C to make the final concentration at 1:300 (w/w) of AgNP:DPPC. The solution was placed in the shaker at 60 °C on 140 rpm for another 20 min after which it was vortexed briefly for 2 min to form multi-lamellar vesicles (MLV). This was then extruded through a 100 nm "Nanosizer" polycarbonate extruder purchased from T&T Scientific (Knoxville, USA). The suspension was subjected to DLS and zeta potential analysis for size and stability measurements respectively.

2.4. Temperature-dependent size measurements, stability tests and pH-dependent drug release study

To check the effect of incubation conditions on the nanocapsules, both probe-sonicated (PB-Lipo-AgNP) and Ex-Lipo-AgNP were subjected to temperature dependent size stability tests. This was done by preparing a solution Lipo-AgNP in 10% fetal bovine serum (FBS) supplemented RPMI-1640 and subjecting them to DLS size measurements over a temperature range of 20 °C–38 °C with 1 °C increments of temperature.

For nanoparticle stability determination, variations in nanoparticles mean size and zeta potential of both Ex-Lipo-AgNP and PB-Lipo-AgNP were measured at a specific interval over a period of 6 months at both 4 °C (storage temperature) and 24 °C (room temperature). 5 mL of PB-Lipo-AgNP and Ex-Lipo-AgNP were incubated at 4 °C and 24 °C and 1 mL sample was taken at each time point for analyses at specific time interval.

For pH dependent AgNP release from the nanocapsules, 1 mL of the encapsulated AgNP was added into a FLOAT-A-LYZER G2 CE dialysis tube with a 1000 KDa MW cut off (Spectrum Labs, Breda, Netherlands). The dialysis tube was placed in 6 mL of either an acetate buffer (pH 6.5) or a phosphate buffer saline (PBS) at pH 7.45. The ratio between the inside and outside volumes were maintained as thus to facilitate easy movement of the AgNP as recommended by Shen and Burgess[11]. The tube was then placed on a shaker running a 300 rpm at 37 °C. To measure the amount of AgNP released, 200 µL of Lipo-AgNP sample was taken from the dialysis tube at specific time interval for 24 h and the absorbance was measured in the SpectraMax M2 microplate reader at 405 nm. After absorbance measurement, the measured sample was replaced with a fresh buffer to avoid change in volume and sink condition.

2.5. Scanning electron micrograph (SEM) and scanning transmission electron micrograph (STEM) analysis

SEM micrographs were obtained for both AgNP and Lipo-AgNPs. Briefly, both PB-Lipo-AgNP and Ex-Lipo-AgNP were microscopically analyzed using Hitachi SU-6600 field emission SEM (Hitachi, Maidenhead, UK) with accelerating voltage of 25 kV and 8 mm working distance. At 24 h before analysis was carried out, 5 µL of sample was drop-cast to air dry onto a 5 × 5 mm pure silicon wafer substrate (Ted Pella Inc., Redding, California, USA) for SEM or carbon formvar copper grid (Agar Scientific Ltd., Stanstead, UK) for STEM, before micrographs were obtained.

2.6. Estimating encapsulation efficiency of the liposome

To estimate the encapsulation efficiency, both probe-sonicated and extruded Lipo-AgNP were centrifuged at 20,000 × *g* for 1 h and the supernatant was harvested. The supernatant was then analyzed by atomic absorption spectrophotometry to estimate the concentration of silver in the solution. The encapsulation efficiency (*E*) of the liposome was then calculated using the formula below

$$E = \frac{Total\ AgNP\ added\ to\ liposome - AgNP\ in\ supernatant}{Total\ AgNP\ added\ to\ liposome} \times 100$$

2.7. Cell culture and alamar blue cell viability

THP1 (ATCC®: TIB-202™) used for this study were cultured in RPMI-1640 media supplemented with 2 mM L-glutamine and 10% FBS. The cells were incubated at 37 °C, 95% humidity and 5% CO_2. For nanoparticle exposure, cells were seeded in a 24-well plate (VWR, Dublin, Ireland) at a density of 3×10^5 cells/mL in media containing 100 ng/mL PMA for a 24 h to induce adherence to the plate. After this, the culture media containing PMA was removed from the now adhered monocytic THP1 cells and replaced with fresh RPMI media containing different concentrations of uncoated AgNP, PB-Lipo-AgNP and Ex-Lipo-AgNP. A positive kill control of cells exposed to dimethyl sulfoxide (DMSO) solution (10% v/v) in RPMI media incorporated onto the plate. A minimum of three independent experiments were conducted and for each independent experiment, four replicate wells were employed per concentration per plate.

To evaluate cell viability post-exposure a pre-warmed 10% AB solution in serum free media was prepared. The exposure media were removed, and the cells were rinsed with prewarmed sterile 1 × phosphate buffer saline (PBS) after which 1.5 mL of AB solution was added onto the cells and incubated at 37 °C for 2 h. The resulting florescence of the converted AB dye was measured at 540 nm excitation and 595 nm emission and excitation wavelengths in a SpectraMax® M2 Multi-Mode Microplate Reader.

2.8. Flow cytometry

THP1 cells were seeded and cultured in T25 flasks at 2×10^5 cells/mL and were subsequently treated with 2 µg/mL of free uncoated AgNP, PB-Lipo-AgNP or Ex-Lipo-AgNP for 24 h. As a positive kill control, THP1 cells exposed to 10% DMSO was also incorporated. After nanoparticle exposure, the cells were harvested into 15 mL tubes and were centrifuged at 300 × g for 5 min at 21 °C. The supernatant was discarded while the pellets were resuspended and rinsed twice in 2 mL prewarmed 1 × PBS and centrifuged. The cells were then resuspended in 1 mL binding buffer containing 0.1% NaN_3 and 1% bovine serum albumin (BSA) solution in 1 × PBS. The cells were double stained with 5 µL of 1 µM calcein-AM stain and 10 µL of 10 µg/mL PI and incubated in the dark at RT for 30 min and analyzed with a BD Accuri C6 flow cytometer.

2.9. Confocal microscopy

THP1 cells were seeded onto a confocal dish (VWR, Dublin Ireland) at density of 3×10^5 cells/mL. The cells were also stimulated with 100 ng/mL of PMA for 24 h and subsequently treated with RPMI media containing 2 µg/mL of either PB-

Table 1. Size and Zeta potential of uncoated AgNP, PB-Lipo-AgNP and Ex-Lipo-AgNP in ddH_2O and RPMI-1640.

	ddH_2O		media	
	Peak 1 (%)	Peak 2 (%)	Peak 1 (%)	Peak 2 (%)
Uncoated AgNP				
DLS Intensity PSD (nm)	21.14 ± 9.48	–	79.15 ± 66.67	–
Zeta (mV)	−26.50	–	−7.90	–
PDI	0.230	–	0.566	–
PB-Lipo-AgNP				
DLS Intensity PSD (nm)	143.7 ± 64.18 (98.7)	5005 ± 605.6 (1.3)	268.7 ± 186.9 (80.4)	2555 ± 1325 (19.6)
Zeta (mV)	−25.9		−0.96	
PDI	0.305		0.437	
Ex-Lipo-AgNP				
DLS Intensity PSD (nm)	140.1 ± 47.49 (100)	N/A	138.9 ± 54.93 (86)	3928 ± 1081 (14)
Zeta (mV)	−31.9		−0.61	
PDI	0.105		0.421	

Lipo-AgNP and Ex-Lipo-AgNP for 24 h. Dish containing cells exposed to 0.5 nM doxorubicin were incorporated as positive kill control. After exposure, the media were discarded, and the cells were rinsed with pre-warmed sterile PBS. The cells were stained with 50 µL of 1 µM calcein-AM and 50 µL of 10 µg/mL PI. The cells were then incubated in the dark at RT for 20 min and rinsed with warm PBS afterwards. Prior to imaging, 1 mL of warm PBS was added onto the cells and imaging was carried out with Zeiss LSM 510 Confocal Laser Scanning Microscope using a Plan-Neofluor oil immersion lens at 40 × magnification and 1.3 numerical aperture.

2.10. Statistical analysis

Statistical analysis was carried out using GraphPad Prism version 7. Data was analyzed by Two-way analysis of variance (ANOVA) with Sidak or Turkey multiple comparisons test to detect significance. Statistically significant differences in tests were indicated for p value < 0.05.

3. Results

3.1. DLS characterization

Results of the DLS characterization of AgNP is summarized in Table 1 for dispersions in water (ddH_2O) and RPMI-1640 culture media. DLS analysis of AgNP shows an increase in mean particle size (MPS) of AgNP when dispersed in ddH_2O to RPMI-1640 media from 21.14 nm to 79.15 nm with polydispersity index (PDI) 0.230–0.566 respectively. The zeta analysis for AgNP in ddH_2O was −26.5 mV which dropped to −7.90 mV in RPMI-1640 media. There was also change in AgNP color from golden yellow in ddH_2O to dark gray when dispersed in RPMI-1640 media which is likely due to agglomeration of the nanoparticle.

3.2. SEM/STEM and spectra analysis of AgNP

SEM analysis of the AgNP showed a spherical nanoparticle with average size of 14.3 ± 1.9 nm (Figure 1A). The UV-Vis spectra of the different AgNP concentration ranging from 0.625 to 10 µg/mL are depicted in Figure 1B, showing a characteristic peak absorption (λmax) corresponding to the surface plasmon resonance (SPR) of 20 nm AgNP at around

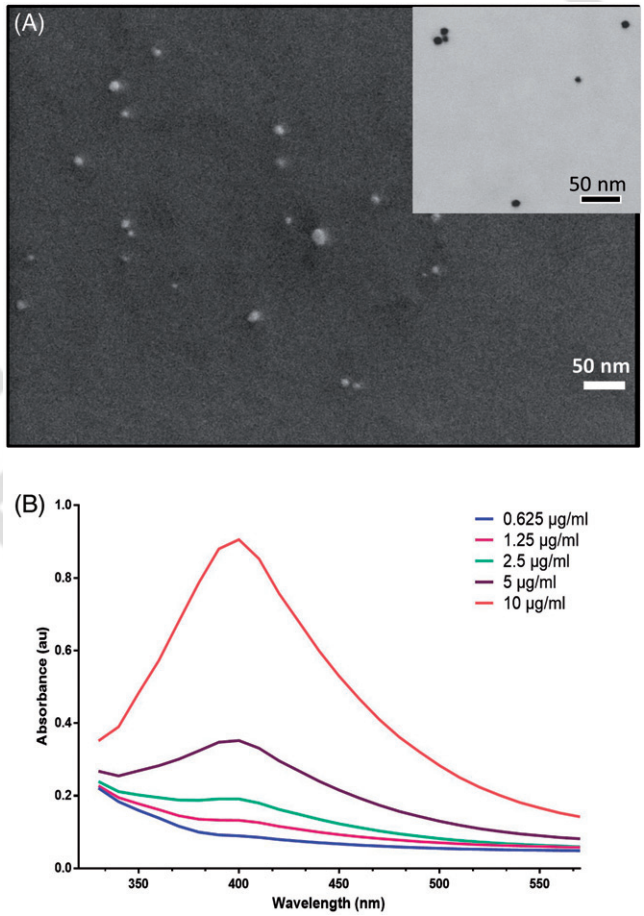

Figure 1. SEM/STEM and UV-Vis Spectra analysis of AgNP (A) SEM and of AgNP with STEM image inset (B) UV spectra analysis of 0.625–10 µg/mL of AgNP measured at 22.6 °C.

400 nm, which was the approximate size obtained by DLS. The peak flattening corresponds to decrease in concentration of AgNP, explained by the reduction in the amount of AgNP particles that absorbs UV light at the wavelengths indicated.

3.3. Liposome characterization

PB-Lipo-AgNP size increased from 143.7 when in ddH_2O to 268.7 nm after dispersion in RPMI-1640 media (Table 1). A second peak of larger sized particles was observed in both ddH2O (1.3%) and RPMI media (19.6%) likely due to agglomeration. The PDI of PB-Lipo-AgNP also increased

from 0.305 to 0.437 after resuspension in RPMI-1640 media but there was a reduction in zeta potential from −25.9 mV in ddH_2O to −0.96 after dispersion in RPMI-1640 media.

For Ex-Lipo-AgNP, there was a small decrease in size from 140.1 nm in ddH_2O to 138.9 nm (half that of PB-Lipo-AgNP) when dispersed in RPMI-1640 media. Unlike the PB-Lipo-AgNP, extrusion produced Lipo-AgNP that was 100% uniform in size in ddH_2O, however, a second peak was found at 3.9 µm for 14% of the particles in RPMI media (Table 1). In contrast, Ex-Lipo-AgNP had a PDI of 0.105 in ddH_2O but this increased to 0.421 in RPMI-1640 media. There was also a reduction in zeta potential of Ex-Lipo-AgNP from −31.9 mV in ddH_2O, higher than that of PB-Lipo-AgNP to −0.61 mV in RPMI-1640.

An overlay of DLS size values of the uncoated AgNP in ddH_2O was carried out with the size values of the PB-Lipo-AgNP obtained with the same AgNP solution both in ddH_2O and in RPMI media (Figure 2C). Overlap in AgNP size value with that of the PB-Lipo-AgNP dispersed in ddH_2O was observed, indicating some of AgNP had not been encapsulated within the PB-Lipo-AgNP. In addition, a shift in the major peak of the PB-Lipo-AgNP was observed for a 120 nm increase in size from dispersion in ddH_2O to RPMI, accounting for 20% of the total nanoparticle. Ex-Lipo-AgNP exhibited no overlap with AgNP in both dispersion media, indicating both nanoparticles have distinct populations (Figure 2D). In addition, there was only a single peak observed for Ex-Lipo-AgNP dispersed in ddH_2O indicative of uniform nanoparticle although there was a slight shift in the major peak to the left as the size reduced by 1.2 nm while a second peak was also visible, accounting for 14% of the total nanoparticle likely due to agglomeration in RPMI.

3.4. UV-Vis spectra analysis of encapsulated AgNP and encapsulation efficiency

Different concentrations of PB-Lipo-AgNP and extruded AgNP, were analyzed by UV-Vis spectra to investigate whether the AgNP has been successfully encapsulated (Figures 3A and 3B). PB-Lipo-AgNP showed a similar spectra characteristic with AgNP especially at 10 µg/mL but there was a red shift in the AgNP peak at around 410 nm, observable for both 5 µg/mL and 10 µg/mL. There was considerable peak flattening at concentration ≤ 5 µg/mL (Figure 3A). It was observed that PB-Lipo-AgNP was cloudy with lipids and retained the golden yellow color of AgNP showing presence of free AgNP (Figure 2A inset). On the contrary for Ex-Lipo-AgNP, the peak absorbance was barely observed even at 10 µg/mL and there was also a red shift in the peak at around 410 nm (Figure 3B). Ex-Lipo-AgNP solution was clear and did not retain the golden yellow color of AgNP (Figure 2B inset), likely because of the refraction due to the lipid layer of the liposome. PB-Lipo-AgNP also had higher absorbance compared to Ex-Lipo-AgNP (at 10 µg/mL) which has similar baseline with uncoated AgNP (Figure 3C), indicating no agglomeration of Ex-Lipo-AgNP. The EE was determined to be 67.8% and 86.5% for the PB-Lipo-AgNP and Ex-Lipo-AgNP respectively, which may explain the similarities between the UV-Vis spectra of free AgNP and PB-Lipo-AgNP since less AgNP was encapsulated.

COLOR Online / B&W in Print

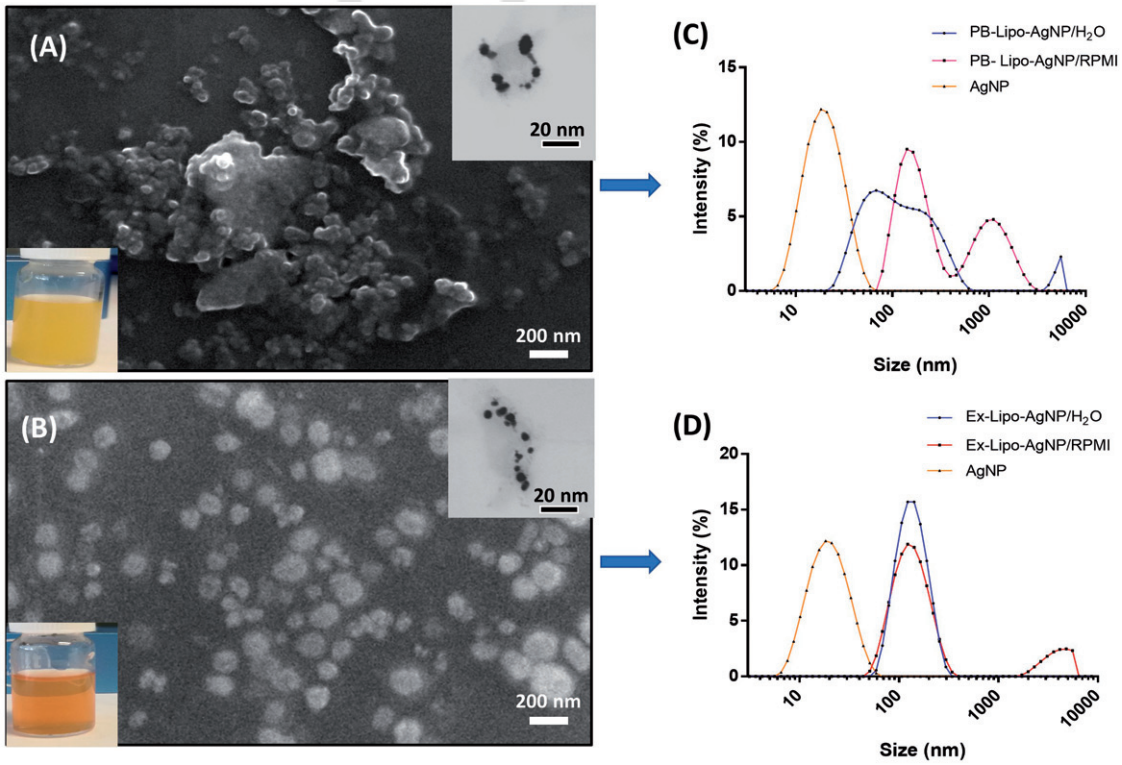

Figure 2. SEM/STEM of PB-Lipo-AgNP and Ex-Lipo-AgNP: (A) SEM with STEM (inset) of PB-Lipo-AgNP, and overlay of AgNP size value with PB-Lipo-AgNP (B) SEM with STEM (inset) Ex-Lipo-AgNP and overlay of AgNP size value with Ex-Lipo-AgNP.

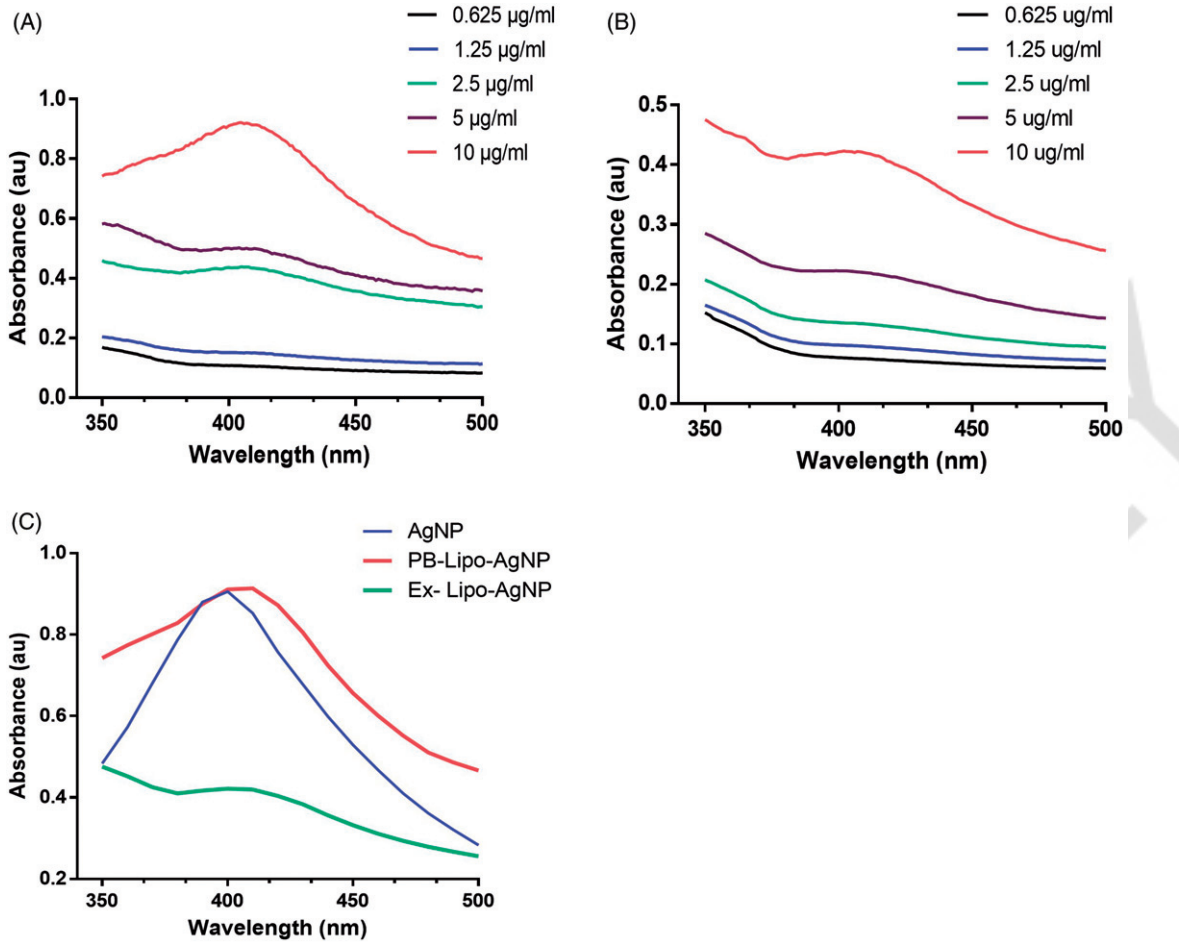

Figure 3. UV-Vis Spectra of PB-Lipo-AgNP and Ex-Lipo-AgNP: UV-Vis spectral analysis of(A) PB-Lipo-AgNP and (B) Ex-Lipo-AgNP at different concentrations between 0.625 µg/mL and 10 µg/mL (C) combined UV-Vis spectra of 10 µg/mL AgNP, Ex-Lipo-AgNP and PB-Lipo-AgNP.

3.5. SEM/STEM analyses of Lipo-AgNP

PB-Lipo-AgNP and Ex-Lipo-AgNP were analyzed microscopically by SEM and STEM (Figures 2A and 2B). As shown, PB-Lipo-AgNP formed agglomerates unlike Ex-Lipo-AgNP. SEM analysis of Ex-Lipo-AgNP showed non-agglomerating spherical liposomes with a well-defined structure. STEM of the PB-Lipo-AgNP (Figure 2A inset) showed AgNP found coated on the liposome with very few nanoparticles encapsulated within. The AgNP in Ex-Lipo-AgNP shown in the STEM (Figure 2B inset) were all encapsulated within the liposome (gray sphere). This alludes to the EE and spectra characteristics of both PB-Lipo-AgNP and Ex-Lipo-AgNP. Size estimation from SEM indicated Ex-Lipo-AgNP was 162.73 ± 29.23 nm while the PB-Lipo-AgNP was 204.22 ± 45.39 nm representing the average of 20 particles counted and similar to the value obtained by DLS.

3.6. Temperature-dependent size change, stability analyses and load release profile of Lipo-AgNP

The practicability of the Lipo-AgNP to retain their contents in *in vitro* experiments was tested under incubation conditions. Sizes of both PB-Lipo-AgNP and Ex-Lipo-AgNP with respect to temperature changes was monitored using DLS in RPMI-1640 media containing 10% FBS over 6 h at 20 min interval for a degree rise in temperature. The initial size of PB-Lipo-AgNP doubled that of Ex-Lipo-AgNP confirming the values in Table 1. PB-Lipo-AgNP size reduced from 334 nm at 20 °C to 150.2 nm, a 55% reduction in size at 37 °C. For Ex-Lipo-AgNP, a reduction from 174.7 nm at 20 °C to 113.1 nm at 37 °C, a 35.3% reduction in size was observed (Figure 4B). This reduction in size could be as result of loss of liposomal content due to increase in temperature.

Stability analyses of the liposomes over a 6-month period is shown in Table 2. After 6 months of incubation, the MPS and zeta potential of PB-Lipo-AgNP increased by 10.3 nm and 5.1 mV respectively at 4 °C. Compared to 4 °C, PB-Lipo-AgNP at 24 °C exhibited a higher reduction in MPS and zeta potential of 19 nm and 4.3 mV for the 6 months in addition to the sedimentation of the lipids that was observed. On the contrary, Ex-Lipo-AgNP showed slight increase in size as well as zeta potential over the 6-month period. At 4 °C, an overall 3.2 nm and 2.0 mV MPS and zeta potential was observed, which was comparable to that observed at 24 °C (5.9 nm and 2.5 mV MPS and zeta potential respectively), and lower to that of PB-Lipo-AgNP for the same time points.

The load release profile of both Lipo-AgNPs was carried out to evaluate AgNP release from the nanocapsule using dialysis. Due to the large volume of fluid outside the dialysis tube and the effect this will have on the absorbance of minute quantity of released nanoparticles from the dialysis

tube, the absorbance of the sample inside of the dialysis tube was measure instead, as drop in absorbance will corresponds to the amount of AgNP released into the buffer. As shown in Figure 5A, PB-Lipo-AgNP appeared to have initial burst release of AgNP as more than 25% of the encapsulated AgNP was released within the first 2 h at pH 6.5. Afterwards, a release of 29% to 30% at 4 and 6 h respectively was observed. Unlike PB-Lipo-AgNP, the extruded AgNP showed a steady release from 2 h up till 6 h, releasing only 15% of the encapsulated AgNP at 6 h, a significantly lower release to that of PB-Lipo-AgNP. Both nanocapsules exhibited similar release at 24 h with PB-Lipo-AgNP releasing 80% of encapsulated AgNP while Ex-Lipo-AgNP released 74%. At physiological pH of 7.45, PB-Lipo-AgNP exhibited lower release rate of AgNP from 2 h to 6 h releasing 0.8% to 12.5% respectively. In the same time point, Ex-Lipo-AgNP only released 0.7% to 3.5% respectively, a significantly lower release than that of PB-Lipo-AgNP. At 24 h, Ex-Lipo-AgNP released 70%, a significantly lower release compared with PB-Lipo-AgNP exhibiting 79% AgNP release (Figure 5B).

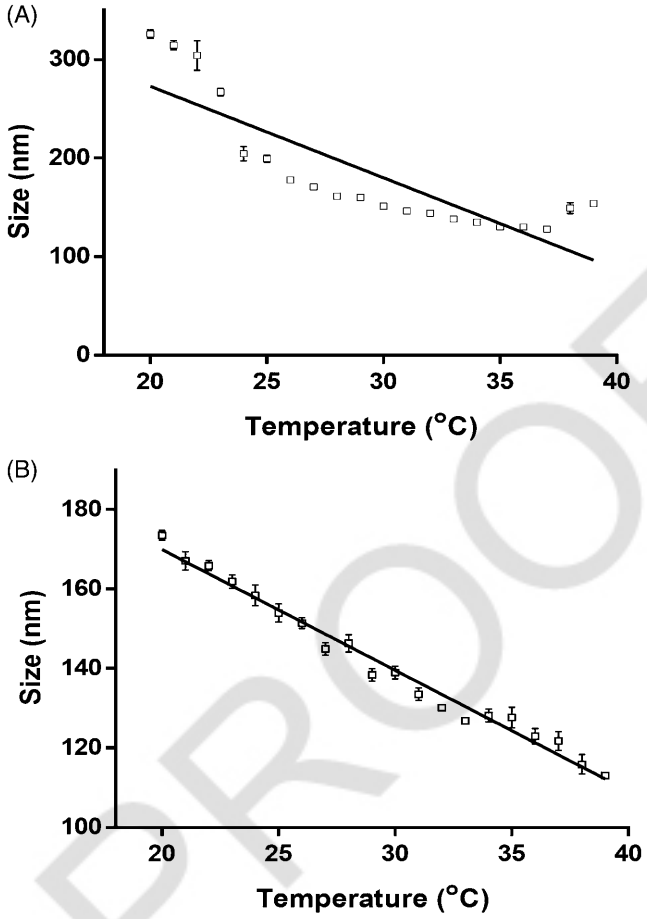

Figure 4. Stability kinetics of probe-sonicated and Ex-Lipo-AgNP: Temperature dependent changes in the sizes of (A) PB-Lipo-AgNP and (B) Ex-Lipo-AgNP dispersed in RPMI-1640 culture medium were analyzed by DLS. Values are mean ± SD from average of three independent measurements.

3.7. Cell viability

To evaluate if the stability of Ex-Lipo-AgNP translates to enhanced cytotoxicity, THP1 cells were first stimulated with 100 ng/mL PMA to induce adherence of the cell line prior to exposure to facilitate easy removal of uninternalized liposome and prevent cell loss during wash steps. After 24 h of exposure to the nanoparticles, viability of the PMA-stimulated THP1 cells was evaluated by their ability to convert the non-fluorescent resazurin in AB dye into a fluorescent resorufin. As shown in Figure 6A, Ex-Lipo-AgNP induced significant reduction in cell viability at concentration ≥ 1.25 µg/mL while uncoated AgNP and PB-Lipo-AgNP induced

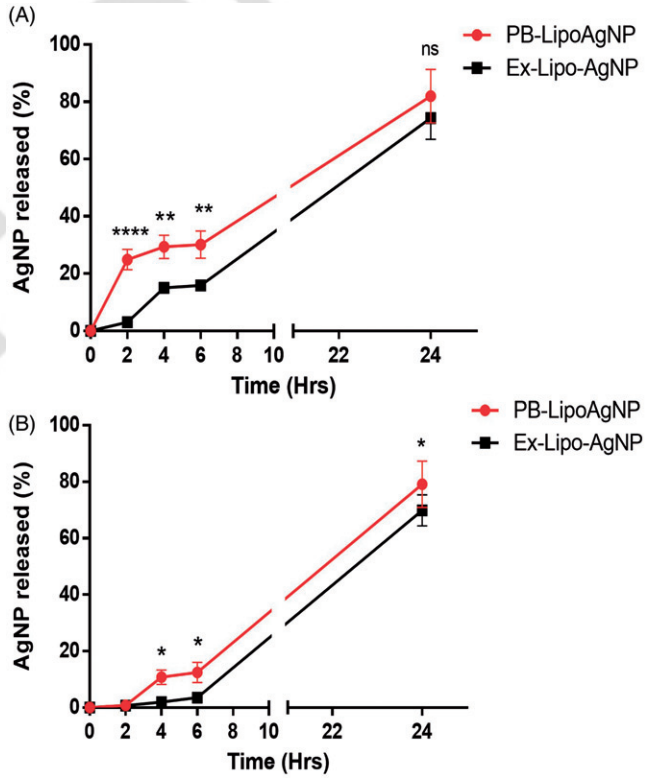

Figure 5. pH dependent drug release profile of PB-Lipo-AgNP and Ex-Lipo-AgNP: Encapsulated AgNP in (A) acetate buffer at pH 6.5 or (B) PBS at pH 7.45 and at specific time interval, 200 µL of the sample was taken out for absorbance measurement. Data is presented as mean ± SD of 3 independent experiments $^{*}p < 0.05$, $^{**}p < 0.01$, $^{****}p < 0.0001$.

Table 2. Stability of PB-Lipo-AgNP and Ex-Lipo-AgNP over a 6-month period.

			Month 1		Month 3		Month 6	
Temp	Initial size (nm)	Initial Zeta (mV)	Size (nm)	Zeta (mV)	Size (nm)	Zeta (mV)	Size (nm)	Zeta (mV)
PB-Lipo-AgNP								
4 °C	143.7 ± 64.18	−25.9	149.44 ± 9.7	−25.5	151 ± 13.3	−24.3	154 ± 20.3	−20.8
24 °C			153.27 ± 9.61	−24.1	156.26 ± 8.9	−23.1	161.34 ± 14.5	−19.6
Ex-Lipo-AgNP								
4 °C	140.1 ± 47.49	−31.9	142.23 ± 3.4	−30.5	144.4 ± 2.5	−30.0	143.33 ± 1.3	−29.9
24 °C			141.33 ± 1.72	−30.9	145 ± 1.98	−30.7	146 ± 2.4	−29.4

COLOR Online / B&W in Print

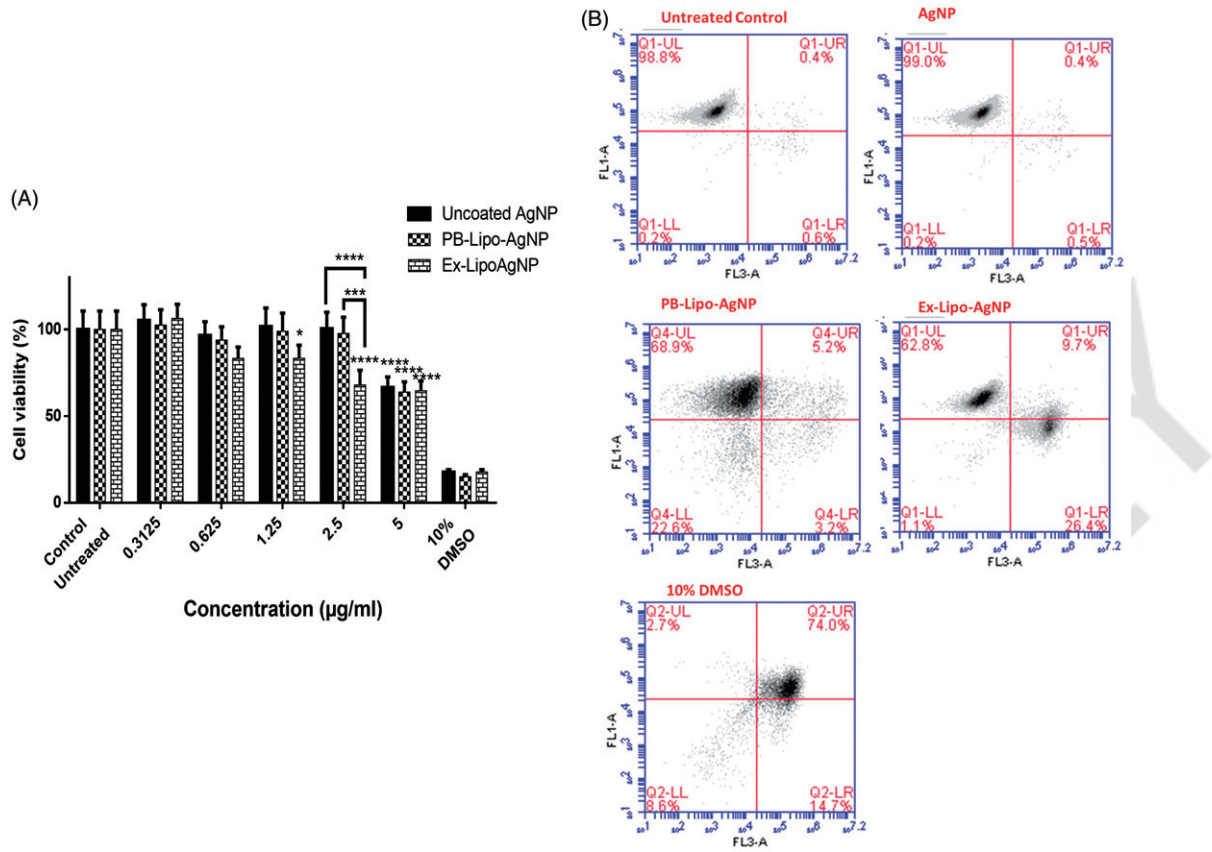

Figure 6. Cell viability of PMA-stimulated THP1 cells post-exposure to AgNP nanocapsules: (A) AB assay determining viability of PMA-stimulated THP1 cells exposed to 0.3–5 µg/mL AgNP, PB-Lipo-AgNP and Ex-Lipo-AgNP for 24 h (B) unstimulated THP1 monocytes cell viability by flow cytometry after exposure to 2 µg/mL of AgNP, PB-Lipo-AgNP and Ex-Lipo-AgNP. Calcein was assessed on FL-1 channel while PI was assessed in the FL-3 channel. Data is presented as mean ± SD of the three independent experiments and similar values were obtained. ***$p < 0.001$ and ****$p < 0.0001$.

significant reduction in the THP1 cell viability at 5 µg/mL. It was observed that Ex-Lipo-AgNP at concentrations of 1.25 and 2.5 µg/mL were significantly more cytotoxic on THP1 cell than the PB-Lipo-AgNP at the same concentration.

A flow cytometry cell viability study was carried out to confirm AB finding since flow cytometry is a more accurate analyses of viability on a cell by cell basis. THP1 monocytes exposed to AgNP, PB-Lipo-AgNP and Ex-Lipo-AgNP were stained with calcein-AM and PI. Calcein-AM is a non-fluorescent stain hydrolyzed by esterase activity of viable cell into a fluorescent calcein derivative that is maintained within cell with intact cell membrane[12], while PI only permeates compromised membrane of dead cells. As expected, Ex-Lipo-AgNP induced significantly more cell death compared to free AgNP and PB-Lipo-AgNP ($p < 0.001$). A significantly higher proportion of early apoptotic cells positive for both calcein and PI (9.7%) and late apoptotic cells that are only positive for PI (26.4%) was observed in Ex-Lipo-AgNP exposed cells compared to unexposed control cells, free AgNP and PB-Lipo-AgNP exposed groups (Figure 6B). In addition to this, PB-Lipo-AgNP exposure resulted in higher proportion of cells identified as cellular debris (22.6%) compared to Ex-Lipo-AgNP (1.1%) which was similar to that in untreated controls and free AgNP exposed cells (0.2%) ($p < 0.001$). This cell population are likely due to PB-Lipo-AgNP identified as cellular debris due to the larger and ununiform sizes.

To further confirm the effect of the Lipo-AgNPs on cell viability, confocal microscopy was used to analyze calcein-AM and PI stained PMA-stimulated THP1 cells exposed to nanocapsules containing equivalent amount of 2 µg/mL AgNP for 24 h. THP1 cells that were exposed to either of PB-Lipo-AgNP or Ex-Lipo-AgNP appeared to have spotted calcein fluorescence (Figures 7A and 7B). This was unlike the control-untreated THP1 cells which appeared to have uniform calcein stain throughout the cytoplasm. In addition, only Ex-Lipo-AgNP induced significantly higher cytotoxicity on THP1 cells compared with control-untreated or PB-Lipo-AgNP exposed cells ($p < 0.01$) (Figures 7A and 7B). Similarly, only Ex-Lipo-AgNP resulted in significantly higher PI fluorescence when compared to both PB-Lipo-AgNP exposed and control-untreated cells ($p < 0.001$). Thus, verifying the result of the AB and flow cytometry assays.

4. Discussion

AgNP can be synthesized from $AgNO_3$ by different methods such as using reducing agents like citrate or $NaBH_4$ with further stabilization of the nanoparticle with compounds such as polyvinyl alcohol (PVA)[13–15]. A citrate-based reduction is most commonly used in the synthesis of AgNP because of its reducing and stabilizing functionality. However, reduction of $AgNO_3$ with citrate results in formation of AgNP in complex with the citrate ions which prevents the release of elemental

COLOR Online / B&W in Print

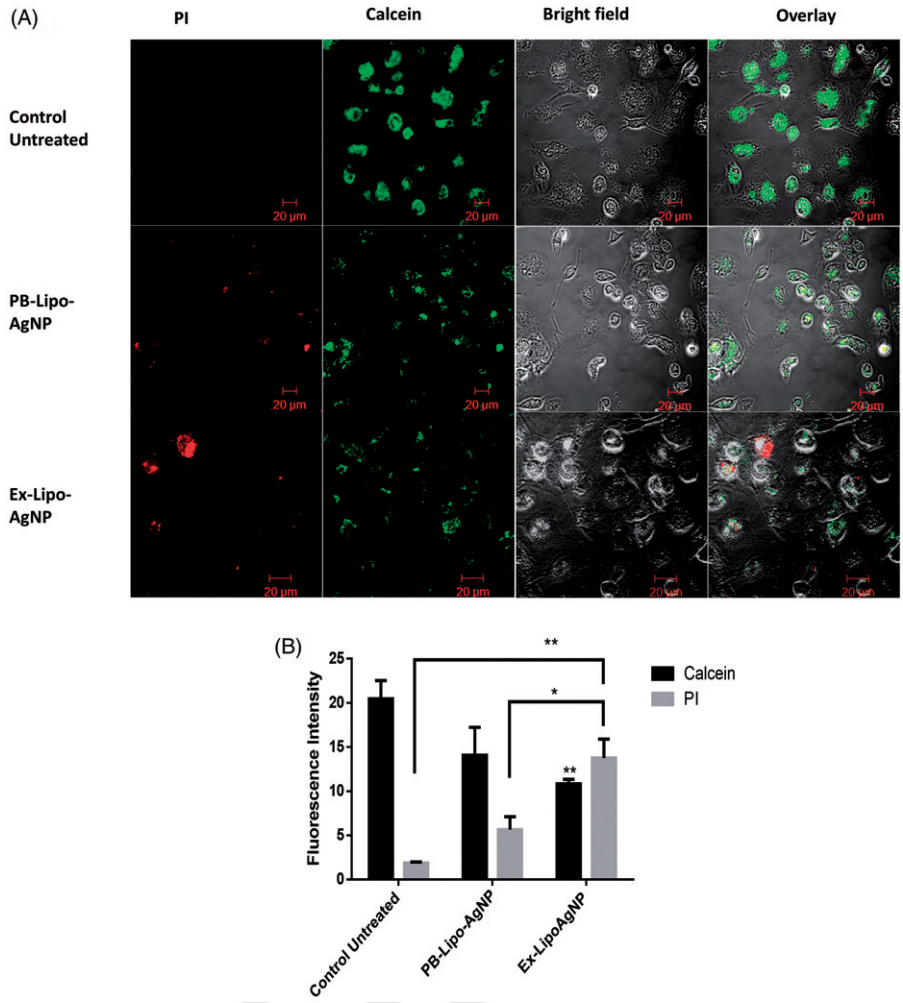

Figure 7. (A) Confocal microscopy assessment of PMA-stimulated THP1 cell viability after exposure to 2 µg/mL of AgNP, PB-Lipo-AgNP and Ex-Lipo-AgNP. Calcein fluorescence is shown in green and PI fluorescence in red (B) fluorescence intensities quantified by ImageJ software from 50 different cells. Data is presented as an abstract value and as mean ± SD of 3 independent experiments. $^{*}p \leq 0.05$ and $^{**}p < 0.01$.

silver[16], limiting its effects. We report here, the encapsulation of AgNP in a DPPC based liposome through different methods to enhance its associated cytotoxicity. The AgNP synthesis employed here was designed to yield elemental AgNP through reduction of $AgNO_3$ by $NaBH_4$ as in the equation below;

$$AgNO_{3(aq)} + NaBH_{4(aq)} \rightarrow Ag^{0}{}_{(s)} + {}^{1}/_{2}B_2H_{6(g)} + {}^{1}/_{2}\ H_{2(g)} + NaNO_{3(aq)}$$

One of the aims of this study was to encapsulate AgNP in a DPPC liposome, as DPPC is a natural biosurfactant in human airways. Thus, it is hoped that such a system will result in a very low capability of inducing adverse immune responses. SEM images of PB-Lipo-AgNP indicated a high agglomeration while that of Ex-Lipo-AgNP indicated a uniform spherical nanoparticle. In addition, DLS analyses indicated higher average size for PB-Lipo-AgNP compared to Ex-Lipo-AgNP both in ddH_2O and RPMI media. It is believed that PB-Lipo-AgNP increased size could have significant impact on cellular response. It is known that larger nanoparticles have reduced bioavailability as they are quickly eradicated by the reticulo-endothelial system[17], making PB-Lipo-AgNP less practical for *in vitro* applications as a drug delivery system. PB-Lipo-AgNP exhibited a lower zeta potential −25.9 mV while that of Ex-Lipo-AgNP was −31.9 mV. Nanoparticles with zeta potential value between −30 and +30 mV are considered less stable owing to the increased agglomeration potential due to reduced repulsion between the particles[18], indicating the Ex-Lipo-AgNP is more stable. In addition to this, the PDI of PB-Lipo-AgNP was found to be higher than that of Ex-Lipo-AgNP in ddH_2O, indicating that Ex-Lipo-AgNP are of more uniform size compared to PB-Lipo-AgNP.

The UV-Vis spectra analysis of free AgNP conformed with reported SPR characteristic of a 20 nm AgNP which is at 400 nm [19], in a way confirming the DLS size of 21 nm. UV-Vis spectra analysis of both PB-Lipo-AgNP and Ex-Lipo-AgNP also allude the success of the encapsulation process. PB-Lipo-AgNP and AgNP had a similar spectra profile with same λmax although PB-Lipo-AgNP spectra exhibited a broadened peak with a raised baseline and a red shift in the λmax, which are indicative of agglomeration/size increase. The λmax also indicates free AgNP that are not successfully encapsulated absorbing UV emission to produce the observed spectrum. In support of this, an overlap in the DLS size value of AgNP with the ddH_2O dispersed PB-Lipo-AgNP observed indicates that the PB-Lipo-AgNP particles in

the overlap region is more likely to be uncoated AgNP. Contrastingly, Ex-Lipo-AgNP spectra depicted a flat peak with same baseline as free AgNP which hints at non-agglomeration of the nanoparticle. The spectra observed at 10 μg/mL was similar to that of 1.25 μg/mL of free AgNP indicating less free AgNP that are able to absorb at the UV-Vis wavelength. This observation is also supported by non-overlap of the AgNP and Ex-Lipo-AgNP DLS size values.

Interaction between nanoparticles and culture media proteins is not uncommon based on their surface reactivity. This interaction was monitored through the size and zeta potential of the liposomes in RPMI-1640 medium. There was increase in the size of PB-Lipo-AgNP and drastic reduction in its zeta potential. The dramatic increase in PB-Lipo-AgNP size in RPMI-1640 could be due to the AgNP on the surface interacting with the proteins in the culture medium as also observed for free AgNP. This is in agreement with the findings of Sabuncu et al.[20] who also reported an increase in gold nanoparticle size and decrease in the zeta potential when dispersed in fetal calf serum (FCS) supplemented DMEM culture. This is supported by the DLS overlay of PB-Lipo-AgNP in ddH_2O and RPMI which indicates increase in size of the nanoparticle from dispersion in ddH_2O to RPMI medium. On the contrary, there was a considerable drop in the zeta potential of Ex-Lipo-AgNP, with only a small increase in the percentage of nanoparticles with increased size (14%). This could mean that Ex-Lipo-AgNP do not readily react with proteins in the culture medium, resulting in no net increase in the size after dispersion in FBS containing RPMI-1640 medium. Interestingly, the charges on the protein amino acids may have a masking effect on Ex-Lipo-AgNP zeta potential. The spectra characteristic of Ex-Lipo-AgNP was less similar to that of AgNP, although with a red shift in λmax at 410 nm. Taken together with the similar baseline as free AgNP and the low absorbance at λmax which is about 50% less than that of free AgNP and PB-Lipo-AgNP, the shift is likely due to the increase in size contributed by the liposome. This also shows that the AgNP is bound to the liposome assuming a larger size than prior to encapsulation such that less AgNP particles are available to interact with proteins in the RPMI media and absorb UV emission. In a study investigating the use of AgNP as biosensor, a red shift in the spectra of a 19 nm AgNP was reported to be consequent upon the binding of the nanoparticle to protein ligands present on the biosensor platform [21], explaining why there was no considerable change in the Lipo-AgNP size in the media.

In temperature dependent study, it was noted that the PB-Lipo-AgNP size decreased by more than half at 37 °C whereas Ex-Lipo-AgNP only decreased in size by about a quarter of the original size. The reason for reduction in their sizes with increased temperature is not known, but this could be as a result of the increased fluidity of the lipid bilayer at temperature close to the transition temperature. Increased fluidity could result in the movement of the liposomal water content out of the liposome into the more concentrated culture medium by osmosis. A previous report indicated liposome often lose their aqueous content when dispersed in medium of high osmolarity[22], such that water moves from region of lower concentration to region of higher concentration through the lipid bilayer. As such, Ex-Lipo-AgNP appeared to be more stable with respect to its ability to retain its content at 37 °C. The stability study over a 6-months period also indicated Ex-Lipo-AgNP to be more stable with minimal overall increase in size and zeta potential at both 4 °C and 24 °C compared to PB-Lipo-AgNP which was also found to sediment unlike the Ex-Lipo-AgNP that remained clear.

Encapsulation of AgNP in liposome here was carried out with the intent of improving its cytotoxicity as a chemotherapeutic agent. Hence, it became pertinent to carry out drug release studies. Considering the possible route of administration and target site for the encapsulated AgNP, pH of 7.45 which is the physiologic pH and most culture media (relevant for *in vitro* studies) and pH 6.5 which is known to be the pH of the tumor microenvironment and inflamed tissue[23–25], were considered. One of the major problems associated with drug delivery systems is the initial burst release which is associated with an initial hypertoxicity and suboptimal concentration of the drug at the time it reaches the target. A good drug delivery system is expected to protect the drug against the harsh physiological environment of immune cells, minimize the burst release and maintain a steady release of the drug for optimal concentration to achieve maximum efficacy over a period. Findings in this study, showed that PB-Lipo-AgNP possesses initial burst release at pH 6.5 and 7.45. Ex-Lipo-AgNP exhibited and maintained a steady release of AgNP at pH 6.5 with significantly lower release compared to PB-Lipo-AgNP. At 24 h, the two systems have released similar concentration of AgNP. At physiologic pH of 7.45, PB-Lipo-AgNP had already released 12.5% of the encapsulated AgNP compared to 3.5% of Ex-Lipo-AgNP. Initial burst release has been demonstrated for Ag^+ coated with titanium dioxide used as an antibacterial for *Staphylococcus aureus*[26]. Although it was found that this rapid release produced an effective antibacterial effect, this effect can be quite adverse in an *in vivo* model.

Initial burst release has been proposed to occur consequent upon rapid dissolution of weakly or poorly encapsulated drugs that might be attached to the surface of the delivery systems[27–30]. This supports our deduction from UV/Vis spectra features of PB-Lipo-AgNP to weakly encapsulate AgNP with some free AgNP attached to the surface of the liposome as also depicted in the STEM image. Contrastingly, our finding indicated that Ex-Lipo-AgNP can maintain steady AgNP release at both pH 6.5 and 7.45. The advantage is that the absence of initial burst release of Ex-Lipo-AgNP prevents initial hypertoxicity. On the other hand, while Ex-Lipo-AgNP had significantly less drug release at 24 h compared with PB-Lipo-AgNP at pH 7.45, stability of Ex-Lipo-AgNP may facilitate better drug delivery with better net cytotoxicity. In support of the finding for Ex-Lipo-AgNP however, Ruttala and Ko [31], showed that a liposomal anti-tumor agent with steady load release exhibited enhanced cytotoxicity.

The uncertainty that encapsulation of AgNP translates to enhanced and improved cytotoxicity led to the investigation of the cytotoxicity of PB-Lipo-AgNP and Ex-Lipo-AgNP on THP1, a leukemic cell line in the monocytic lineage. The choice of the cell line for this study is three-folds. Firstly, THP1 is a leukemic (cancer) cell line, allowing investigation of the cytotoxic effect of AgNP encapsulation on a cancer cell line. Secondly, monocytes and similar immune cells act as first line of Defense in response to foreign objects including nanoparticles upon human exposure[32–34], making the cell line a perfect model to also study the effect of the nanoparticle on the innate immune system. In addition to this, due to the role of monocytes in diseases such as atherosclerosis and cancer[35], this cell line is a potential therapeutic target in treatment of this diseases.

Upon exposure of THP1 monocytes to the different nanoparticles, it was discovered that Ex-Lipo-AgNP induced significantly higher cytotoxicity at lower concentrations compared with PB-Lipo-AgNP and free uncoated AgNP exposed cells. In addition, flow cytometry and confocal microscopy analyses both confirmed Ex-Lipo-AgNP to be more cytotoxic compared to PB-Lipo-AgNP and free uncoated AgNP. There was a significantly higher live cells and less dead cells in the control-untreated, free uncoated AgNP, and PB-Lipo-AgNP exposed cells groups compared to Ex-Lipo-AgNP exposed cells. Another observation was the speckled fluorescence observed in both PB-Lipo-AgNP and Ex-Lipo-AgNP exposed cells but not the control-untreated cells. This is likely due to the loss of membrane integrity upon exposure to the nanoparticles resulting in leakage of calcein from the cytoplasm. Foged et al.[36] have previously showed that disruption of the cell membrane can result in leakage of calcein.

The enhanced cytotoxicity of Ex-Lipo-AgNP in comparison to AgNP or PB-Lipo-AgNP may be attributed to its superior characteristics and enhanced delivery. This may have been facilitated by the hydrophobic interaction between the lipid bilayer of the cell membrane and that of the liposome encapsulating the AgNP. On the other hand, the slightly enhanced cytotoxicity of the PB-Lipo-AgNP may be because of less encapsulated AgNP and lower endocytosis due to larger size in culture media. This reason may also explain why Ex-Lipo-AgNP enhanced delivery into the cells since its size may have remained unchanged even when reconstituted in culture media. Lastly, flow cytometry detected more cellular debris in PB-Lipo-AgNP exposed THP1 cells than in other exposure groups. These debris were due to the PB-Lipo-AgNP which were larger in size and similar to left over of apoptosed cells. Unfortunately, this identified debris are counted as events in the cytometer, imposing a confounding effect on the number of viable cells that will be analyzed. Interestingly, Ex-Lipo-AgNP does not exhibit such anomaly, further alluding to the stability and superior characteristic liposome obtained through the extrusion as compared with that obtained from probe sonication. Taken together, encapsulation of AgNP in DPPC based liposome may help limit the concentration of AgNP used in the various biomedical applications to achieve better cytotoxicity resulting in less human exposure and mitigation of any development of adverse effects.

5. Conclusion

Stable AgNP were successfully synthesized at a suitable concentration without the need for stabilizer. Synthesized AgNP were successfully encapsulated in liposome for the first time by both probe sonication and extrusion methods. However, the extrusion method produced a more stable liposome both when dispersed in ddH_2O and in culture medium. The spectra analysis confirms probe sonication produced a less successful encapsulation based on the similarity between PB-Lipo-AgNP and AgNP spectra characteristics. Ex-Lipo-AgNP on the other hand had a different spectra analysis which is believed to be as a result of the shielding effect of the liposome bilayer. In addition, Ex-Lipo-AgNP exhibited a more controlled AgNP release compared with the PB-Lipo-AgNP which showed an initial burst release. Cell viability studies indicated that Ex-Lipo-AgNP exhibited higher cytotoxic effect in comparison to PB-Lipo-AgNP and uncoated AgNP at similar concentrations. This may have been due to the stable characteristic of Ex-Lipo-AgNP facilitating an effective delivery of the nanoparticle into the cell. As such, extrusion method offers a more reliable way for encapsulating AgNP in liposome with repetitive characteristics and enhanced cytotoxicity. This provides with potential of achieving cytotoxicity at lower concentrations compared to those currently in application limiting possible exposures.

Disclosure statement

No potential conflict of interest was reported by the authors.

Funding

This research work and Azeez Yusuf was supported by the Dublin Institute of Technology's Fiosraigh dean of graduate's research fellowship. Alan Casey acknowledges the support of the Science Foundation Ireland Principal Investigator Award 11/PI/1108.

References

[1] Polivkova, M.; Hubacek, T.; Staszek, M.; Svorcik, V.; Siegel, J. Antimicrobial Treatment of Polymeric Medical Devices by Silver Nanomaterials and Related Technology. *Int. J. Mol. Sci.* **2017**, *18*, pii: E419.

[2] Carbone, M.; Donia, D. T.; Sabbatella, G.; Antiochia, R. Silver Nanoparticles in Polymeric Matrices for Fresh Food Packaging. *J. King Saud Univ. – Sci.* **2016**, *28*, 273–279. DOI: 10.1016/j.jksus.2016.05.004.

[3] Asharani, P.; Sethu, S.; Lim, H. K.; Balaji, G.; Valiyaveettil, S.; Hande, M. P. Differential Regulation of Intracellular Factors Mediating Cell Cycle, DNA Repair and Inflammation following Exposure to Silver Nanoparticles in Human Cells. *Genome Integr.* **2012**, *3*, 2. DOI: 10.1186/2041-9414-3-2.

[4] Juarez-Moreno, K.; Gonzalez, E. B.; Giron-Vazquez, N.; Chavez-Santoscoy, R. A.; Mota-Morales, J. D.; Perez-Mozqueda, L. L.; Garcia-Garcia, M. R.; Pestryakov, A.; Bogdanchikova, N. Comparison of Cytotoxicity and Genotoxicity Effects of Silver

Nanoparticles on Human Cervix and Breast Cancer Cell Lines. *Hum. Exp. Toxicol.* **2017**, *36*, 931–948. DOI: 10.1177/0960327116675206.

[5] Foldbjerg, R.; Dang, D. A.; Autrup, H. Cytotoxicity and Genotoxicity of Silver Nanoparticles in the Human Lung Cancer Cell Line, A549. *Arch. Toxicol.* **2011**, *85*, 743–750. DOI: 10.1007/s00204-010-0545-5.

[6] Foldbjerg, R.; Irving, E. S.; Hayashi, Y.; Sutherland, D. S.; Thorsen, K.; Autrup, H.; Beer, C. Global Gene Expression Profiling of Human Lung Epithelial Cells after Exposure to Nanosilver. *Toxicol. Sci.* **2012**, *130*, 145–157. DOI: 10.1093/toxsci/kfs225.

[7] León-Silva, S.; Fernández-Luqueño, F.; López-Valdez, F. Silver Nanoparticles (AgNP) in the Environment: A Review of Potential Risks on Human and Environmental Health. *Water, Air, Soil Pollut.* **2016**, *227*, 306. DOI: 10.1007/s11270-016-3022-9.

[8] Agassandian, M.; Mallampalli, R. K. Surfactant Phospholipid Metabolism. *Biochim. Biophys. Acta* **2013**, *1831*, 612–625. DOI: 10.1016/j.bbalip.2012.09.010.

[9] Briuglia, M. L.; Rotella, C.; McFarlane, A.; Lamprou, D. A. Influence of Cholesterol on Liposome Stability and on In Vitro Drug Release. *Drug Deliv. Transl. Res.* **2015**, *5*, 231–242. DOI: 10.1007/s13346-015-0220-8.

[10] Wu, Q.; Jin, R.; Feng, T.; Liu, L.; Yang, L.; Tao, Y.; Anderson, J. M.; Ai, H.; Li, H. Iron Oxide Nanoparticles and Induced Autophagy in Human Monocytes. *Int. J. Nanomed.* **2017**, *12*, 3993–4005. DOI: 10.2147/IJN.S135189.

[11] Shen, J.; Burgess, D. J. In Vitro Dissolution Testing Strategies for Nanoparticulate Drug Delivery Systems: Recent Developments and Challenges. *Drug Deliv. And Transl. Res.* **2013**, *3*, 409–415. DOI: 10.1007/s13346-013-0129-z.

[12] Uggeri, J.; Gatti, R.; Belletti, S.; Scandroglio, R.; Corradini, R.; Rotoli, B. M.; Orlandini, G. Calcein-AM Is a Detector of Intracellular Oxidative Activity. *Histochem. Cell Biol.* **2000**, *122*, 499–505. DOI: 10.1007/s00418-004-0712-y.

[13] Becaro, A. A.; Jonsson, C. M.; Puti, F. C.; Siqueira, M. C.; Mattoso, L. H.; Correa, D. S.; Ferreira, M. D. Toxicity of PVA-Stabilized Silver Nanoparticles to Algae and Microcrustaceans. *Environ. Nanotechnol. Monit. Manage.* **2015**, *3*, 22–29. DOI: 10.1016/j.enmm.2014.11.002.

[14] Cheon, J. Y.; Kang, Y. O.; Park, W. H. Formation of Ag Nanoparticles in PVA Solution and Catalytic Activity of Their Electrospun PVA Nanofibers. *Fibers Polym.* **2015**, *16*, 840–849. DOI: 10.1007/s12221-015-0840-0.

[15] Dong, X.; Ji, X.; Wu, H.; Zhao, L.; Li, J.; Yang, W. Shape Control of Silver Nanoparticles by Stepwise Citrate Reduction. *J. Phys. Chem. C* **2009**, *113*, 6573–6576. DOI: 10.1021/jp900775b.

[16] Djokic, S. Synthesis and Antimicrobial Activity of Silver Citrate Complexes. *Bioinorg. Chem. Appl.* **2008**, *2008*, 436458.

[17] Maruyama, K. Intracellular Targeting Delivery of Liposomal Drugs to Solid Tumors Based on EPR Effects. *Adv. Drug Deliv. Rev.* **2011**, *63*, 161–169. DOI: 10.1016/j.addr.2010.09.003.

[18] Shieh, Y. T.; Chen, J. Y.; Twu, Y. K.; Chen, W. J. The Effect of pH and Ionic Strength on the Dispersion of Carbon Nanotubes in Poly (Acrylic Acid) Solutions. *Polym. Int.* **2012**, *61*, 554–559. DOI: 10.1002/pi.3203.

[19] Zuber, A.; Purdey, M.; Schartner, E.; Forbes, C.; van der Hoek, B.; Giles, D.; Abell, A.; Monro, T.; Ebendorff-Heidepriem, H. Detection of Gold Nanoparticles with Different Sizes Using Absorption and Fluorescence Based Method. *Sens. Actuat. B: Chem.* **2016**, *227*, 117–127. DOI: 10.1016/j.snb.2015.12.044.

[20] Sabuncu, A. C.; Grubbs, J.; Qian, S.; Abdel-Fattah, T. M.; Stacey, M. W.; Beskok, A. Probing Nanoparticle Interactions in Cell Culture Media. *Colloids Surf. B Biointerfaces* **2012**, *95*, 96–102. DOI: 10.1016/j.colsurfb.2012.02.022.

[21] Liao, W. S.; Chen, X.; Yang, T.; Castellana, E. T.; Chen, J.; Cremer, P. S. Benchtop Chemistry for the Rapid Prototyping of Label-Free Biosensors: Transmission Localized Surface Plasmon Resonance Platforms. *Biointerphases* **2009**, *4*, 80–85. DOI: 10.1116/1.3284738.

[22] Monteiro, N.; Martins, A.; Reis, R. L.; Neves, N. M. Liposomes in Tissue Engineering and Regenerative medicine. *J. R. Soc. Interface* . **2014**, *11*, 20140459.DOI: 10.1098/rsif.2014.0459.

[23] Ueno, T.; Tsuchiya, H.; Mizogami, M.; Takakura, K. Local Anesthetic Failure Associated with Inflammation: verification of the Acidosis Mechanism and the Hypothetic Participation of Inflammatory Peroxynitrite. *J. Inflamm. Res.* **2008**, *1*, 41–48.

[24] Huber, V.; Camisaschi, C.; Berzi, A.; Ferro, S.; Lugini, L.; Triulzi, T.; Tuccitto, A.; Tagliabue, E.; Castelli, C.; Rivoltini, L.; et al. Cancer Acidity: An Ultimate Frontier of Tumor Immune Escape and a Novel Target of Immunomodulation. *Semin. Cancer Biol.* **2017**, *43*, 74–89. DOI: 10.1016/j.semcancer.2017.03.001.

[25] Som, A.; Bloch, S.; Ippolito, J. E.; Achilefu, S. Acidic Extracellular pH of Tumors Induces Octamer-Binding Transcription Factor 4 Expression in Murine Fibroblasts in Vitro and in Vivo. *Sci. Rep.* **2016**, *6*, 27803. DOI: 10.1038/srep27803.

[26] Jamuna-Thevi, K.; Bakar, S.; Ibrahim, S.; Shahab, N.; Toff, M. Quantification of Silver Ion Release, In Vitro Cytotoxicity and Antibacterial Properties of Nanostuctured Ag Doped TiO2 Coatings on Stainless Steel Deposited by RF Magnetron Sputtering. *Vacuum*. **2011**, *86*, 235–241. DOI: 10.1016/j.vacuum.2011.06.011.

[27] Rivadeneira, J.; Di Virgilio, A.; Audisio, M.; Boccaccini, A.; Gorustovich, A. Evaluation of Antibacterial and Cytotoxic Effects of Nano-Sized Bioactive Glass/Collagen Composites Releasing Tetracycline Hydrochloride. *J. Appl. Microbiol.* **2014**, *116*, 1438–1446. DOI: 10.1111/jam.12476.

[28] Hua, X.; Tan, S.; Bandara, H. M.; Fu, Y.; Liu, S.; Smyth, H. D. Externally Controlled Triggered-Release of Drug from PLGA Micro and Nanoparticles. *PLoS One* **2014**, *9*, e114271. DOI: 10.1371/journal.pone.0114271.

[29] Singh, R.; Lillard, J. W. Nanoparticle-Based Targeted Drug Delivery. *Exp. Mol. Pathol.* **2009**, *86*, 215–223. DOI: 10.1016/j.yexmp.2008.12.004.

[30] Tan, J. M.; Karthivashan, G.; Arulselvan, P.; Fakurazi, S.; Hussein, M. Z. Sustained Release and Cytotoxicity Evaluation of Carbon Nanotube-Mediated Drug Delivery System for Betulinic Acid. *J. Nanomater.* **2014**, *2014*, 1. DOI: 10.1155/2014/862148.

[31] Ruttala, H. B.; Ko, Y. T. Liposome Encapsulated Albumin-Paclitaxel Nanoparticle for Enhanced Antitumor Efficacy. *Pharm. Res.* **2015**, *32*, 1002–1016. DOI: 10.1007/s11095-014-1512-2.

[32] Mrakovcic, M.; Meindl, C.; Roblegg, E.; Frohlich, E. Reaction of Monocytes to Polystyrene and Silica Nanoparticles in short-term and long-term exposures . *Toxicol. Res. (Camb)* **2014**, *3*, 86–97. DOI: 10.1039/C3TX50112D.

[33] Rueda-Romero, C.; Hernandez-Perez, G.; Ramos-Godinez, P.; Vazquez-Lopez, I.; Quintana-Belmares, R. O.; Huerta-Garcia, E.; Stepien, E.; Lopez-Marure, R.; Montiel-Davalos, A.; et al. Titanium Dioxide Nanoparticles Induce the Expression of Early and Late Receptors for Adhesion Molecules on Monocytes. *Part Fibre Toxicol.* **2016**, *13*, 36.

[34] Robbins, G. R.; Roberts, R. A.; Guo, H.; Reuter, K.; Shen, T.; Sempowski, G. D.; McKinnon, K. P.; Su, L.; DeSimone, J. M.; Ting, J. P.-Y.; et al. Analysis of Human Innate Immune Responses to PRINT Fabricated Nanoparticles with Cross Validation Using a Humanized Mouse Model. *Nanomed. Nanotechnol. Biol. Med.* **2015**, *11*, 589–599. DOI: 10.1016/j.nano.2014.11.010.

[35] Lameijer, M. A.; Tang, J.; Nahrendorf, M.; Beelen, R. H. J.; Mulder, W. J. M. Monocytes and Macrophages as Nanomedicinal Targets for Improved Diagnosis and Treatment of Disease. *Expert Rev. Mol. Diagn.* **2013**, *13*, 567–580. DOI: 10.1586/14737159.2013.819216.

[36] Foged, C.; Franzyk, H.; Bahrami, S.; Frokjaer, S.; Jaroszewski, J. W.; Nielsen, H. M.; Olsen, C. A. Cellular Uptake and Membrane-Destabilising Properties of Alpha-Peptide/Beta-Peptoid Chimeras: Lessons for the Design of New Cell-Penetrating Peptides. *Biochim. Biophys. Acta* **2008**, *1778*, 2487–2495. DOI: 10.1016/j.bbamem.2008.06.020.